EPJ C manuscript No.
(will be inserted by the editor)

LU 2003/004, LPNHE 2003-03

New method for calculating helicity amplitudes of jet-like QED processes for high-energy colliders

II. Processes with lepton pair production

C. Carimalo[1a], A. Schiller[2,b], and V.G. Serbo[3,c]

[1] LPNHE, IN2P3-CNRS, Université Paris VI, F-75252 Paris, France
[2] Institut für Theoretische Physik and NTZ, Universität Leipzig, D-04109 Leipzig, Germany
[3] Novosibirsk State University, Novosibirsk, 630090 Russia

March 31, 2003

Abstract. As continuation of our previous paper [1] we further develop our new method for calculating helicity amplitudes of jet-like QED processes described by tree diagrams, applying it to lepton pair production. This method consists in replacing spinor structures for real and weakly virtual intermediate leptons by simple transition vertices. New vertices are introduced for the pair production case, and previous bremsstrahlung vertices are generalized to include virtual photons inside the considered jet. We present a diagrammatic approach that allows to write down in an efficient way the leading helicity amplitudes, at tree level. The obtained compact amplitudes are particularly suitable for numerical calculations in jet-like kinematics. Several examples with up to four particles in a jet are discussed in detail.

1 Introduction

In paper [1] we have studied quantum electrodynamics (QED) bremsstrahlung processes[1]

$$e(p_1)+e^{\pm}(p_2)\to e(p_3)+\gamma(k_1)+\ldots+\gamma(k_n)+e^{\pm}(p_4) \quad (1)$$

in the jet-like kinematics: $E_i \gg m$ and $m \lesssim |\mathbf{p}_{i\perp}| \ll E_i$ including the helicities of all particles. In particular, we have considered in detail the emission of one, two and three photons along the direction of the first initial lepton described by the block diagrams of Figs. 1.2, 1.9 and 1.11, respectively. The corresponding amplitudes have the form

$$M_{fi} = \frac{s}{q^2} J_1 J_2 \quad (2)$$

where the impact factors J_1 for the different bremsstrahlung processes in the first jet have been found in Sections 4, 5 and 6 of that paper, while the second (trivial) impact factor for reaction (1) is

$$J_2 = \mp\sqrt{8\pi\alpha}\,\delta_{\lambda_2\lambda_4}\,\mathrm{e}^{\mathrm{i}(\lambda_2\varphi_2-\lambda_4\varphi_4)}\,. \quad (3)$$

The main idea of our approximation consists in replacing the numerators of the lepton propagators of small virtuality by vertices which are matrices with respect to lepton helicities. These vertices $V(p,k)$, $\widetilde{V}(p,k)$ and $V(p)$ are simple analytical expressions given in Sect. 3.1 of [1] and they represent the building blocks for the whole amplitude of the bremsstrahlung processes.

In the present paper we consider processes with lepton pair production. All nontrivial points can be demonstrated considering the pair production processes of order e^3 and e^4.

To order e^3 there is one process for the photo-production of a single lepton pair (Fig. 1.3). The corresponding impact factor can be easily obtained from the impact factor for the single bremsstrahlung of Fig. 1.2 by a transition to the cross-channel. Performing that transformation for the impact factor J_1, all amplitudes for the processes of Figs. 1.4–1.6 are given as simple combinations of the obtained impact factors.

Among the other processes of order e^4 mentioned in paper [1], only the bremsstrahlung pair production (Fig. 1.8) can be considered as a new process, since diagrams of Figs. 1.7 and 1.10 represent amplitudes which are the cross-channel amplitudes for the direct processes of Figs. 1.8 and 1.9, respectively.

Therefore, we have to calculate the impact factor for the bremsstrahlung pair production of Fig. 1.8 and to find out the substitution rules for energy fractions, transverse momenta and polarizations of the particles under crossing. In the calculation additional vertices will be introduced and the bremsstrahlung vertices of our previous paper have to be generalized including virtual photons with helicity zero.

[a] carimalo@in2p3.fr
[b] Arwed.Schiller@itp.uni-leipzig.de
[c] serbo@math.nsc.ru

[1] Below we shall quote formulae and figures from this paper by a double numbering, for example, Eq. (1.21) and Fig. 1.3 means Eq. (21) and Fig. 3 from Ref. [1]. For a more complete list of references consult our previous work.

Those vertices as well as the rules for crossing are presented in Sect. 2. In Sect. 3 we derive the impact factor of Fig. 1.3 using the crossing relations which is the basis for pair production in γe and $\gamma\gamma$ collisions. In the next Section we consider the bremsstrahlung pair production of Fig. 1.8. Here for the first time intermediate virtual photons have to be taken into account in the considered jet. This represents the starting point for considering more complicated processes in the jet-like kinematics. As an example illustrating the efficiency of the new method we consider in Sect. 5 its application to the more complicated process of Fig. 1 — the collision of an electron and a positron with production of a $\mu^+\mu^-$ pair together with a photon inside the first jet. Our results are summarized in the final section.

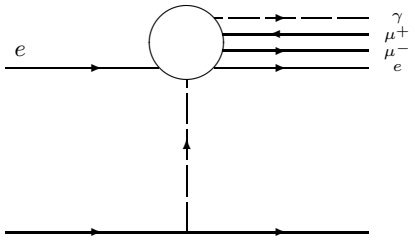

Fig. 1. The block diagram for the process $ee \to ee\mu^+\mu^-\gamma$

2 Method for calculation of amplitudes with pair production

In addition to formulae presented in Sect. 2 of [1], we derive in this section some additional rules and formulae useful for processes with lepton pair production.

2.1 Vertices related to pair production

In this subsection we consider the new vertices appearing in the processes described by Figs. 1.3, 1.5–1.8, 1.10 and Fig. 1. For jet-like processes with lepton pair production we can repeat the main points from [1]. In particular, we present the amplitude M_{fi} in the factorized form (2). Then, we express the numerators of all spinor propagators $\hat{p} \pm m$ with $E > 0$ for virtual $e^{\mp}$ via bispinors for real electrons and positrons with 3-momentum $\mathbf{p}$ or $(-\mathbf{p})$:

$$\hat{p} + m = u^{(\lambda)}_{\mathbf{p}} \bar{u}^{(\lambda)}_{\mathbf{p}} + \frac{p^2 - m^2}{4E^2}\, v^{(\lambda)}_{-\mathbf{p}} \bar{v}^{(\lambda)}_{-\mathbf{p}}\,, \qquad (4)$$

$$\hat{p} - m = v^{(\lambda)}_{\mathbf{p}} \bar{v}^{(\lambda)}_{\mathbf{p}} + \frac{p^2 - m^2}{4E^2}\, u^{(\lambda)}_{-\mathbf{p}} \bar{u}^{(\lambda)}_{-\mathbf{p}}\,.$$

This allows us to replace $\hat{p} \pm m$ by transition currents or generalized vertices with real electrons and positrons. In addition to the vertices $V(p,k)$, $\widetilde{V}(p,k)$ and $V(p)$ for bremsstrahlung given in (1.37)–(1.43), we have to consider now new vertices for the bremsstrahlung of a virtual photon as well as vertices for the transition $\gamma(k) \to e^+(p_+) + e^-(p_-)$ where $\gamma(k)$ is a real or virtual photon with 4-momentum k.

To illustrate this point, let us consider, for example, the bremsstrahlung $\mu^-\mu^+$ production of Fig. 1.8

$$e^- + e^+ \to e^-\mu^-\mu^+ + e^+\,.$$

We present the impact factor of this process, described

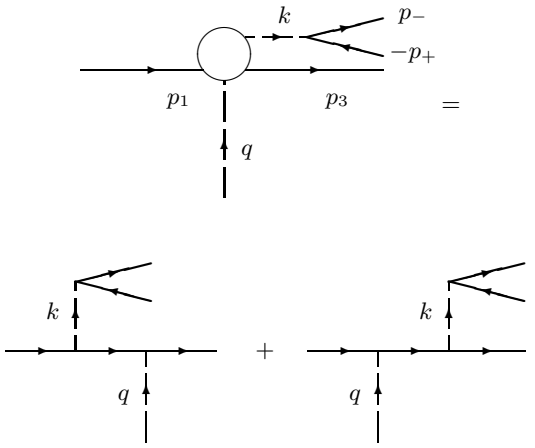

Fig. 2. Feynman diagrams for the impact factor related to bremsstrahlung $\mu^+\mu^-$ pair production

by Feynman diagrams of Fig. 2, in the form

$$J_1(e^-_{\lambda_1} + \gamma^* \to e^-_{\lambda_3} + \mu^+_{\lambda_+} + \mu^-_{\lambda_-}) = \frac{\sqrt{4\pi\alpha}}{k^2}\, A_\mu I^\mu\,, \qquad (5)$$

where I^μ is the current for the virtual transition $\gamma(k) \to \mu^+(p_+) + \mu^-(p_-)$,

$$I^\mu = \bar{u}^{(\lambda_-)}_{\mathbf{p}_-}\, \gamma^\mu\, v^{(\lambda_+)}_{\mathbf{p}_+}\,, \qquad (6)$$

and A^μ is the amplitude of the virtual Compton scattering,

$$A^\mu = 4\pi\alpha \left(\frac{N_1^\mu}{2p_1k - k^2} - \frac{N_3^\mu}{2p_3k + k^2} \right)\,, \qquad (7)$$

$$N_1^\mu = \bar{u}_3\, \hat{e}_q\, (\hat{p}_1 - \hat{k} + m)\gamma^\mu u_1\,,$$
$$N_3^\mu = \bar{u}_3 \gamma^\mu (\hat{p}_3 + \hat{k} + m)\, \hat{e}_q\, u_1\,.$$

The 4-vector

$$e_q \equiv \frac{\sqrt{2}P_2}{s} \qquad (8)$$

can be considered as an "effective polarization vector" for the t-channel virtual photon with momentum q.

Both 4-vectors A^μ and I^μ are orthogonal to the momentum of the virtual photon k due to gauge invariance:

$$Ak = Ik = 0\,.$$

Therefore, A^μ and I^μ have only three independent components which can be chosen along the three polarization

4-vectors $e^{(\Lambda)}(k)$ for the virtual photon with 4-momentum k and helicity $\Lambda = 0, \pm 1$:

$$e^{(\pm)}(k) = e_\perp^{(\pm)} - \frac{k e_\perp^{(\pm)}}{kP_2}\, P_2\,, \tag{9}$$

$$e_\perp^{(\pm)} = \mp\frac{1}{\sqrt{2}}\,(0,\, 1,\, \pm\mathrm{i},\, 0)\,,$$

$$e^{(0)}(k) = \frac{\sqrt{k^2}}{kP_2}\left(P_2 - \frac{kP_2}{k^2}\,k\right)\,. \tag{10}$$

These vectors obey the conditions:

$$k\,e^{(\Lambda)} = 0\,,\;\; e^{(\Lambda)*}e^{(\Lambda')} = -\delta_{\Lambda\Lambda'}\,,$$

$$\sum_{\Lambda=0,\,\pm1} e_\mu^{(\Lambda)*} e_\nu^{(\Lambda)} = -g_{\mu\nu} + \frac{k_\mu k_\nu}{k^2}\,. \tag{11}$$

Due to gauge invariance, we can use $e^{(0)}$ in the simpler form

$$e^{(0)}(k) = \frac{\sqrt{k^2}}{kP_2}\,P_2\,. \tag{12}$$

Note, that this vector is quite similar to the vector $e_q = \sqrt{2}P_2/s$. The last equation in (11) allows us to replace the scalar product AI by the sum over helicity states of the virtual photon

$$AI = -\sum_{\Lambda=0,\,\pm1} A^{(\Lambda)} I^{(\Lambda)}\,, \tag{13}$$

$$A^{(\Lambda)} = A\,e^{(\Lambda)*}\,,\quad I^{(\Lambda)} = I\,e^{(\Lambda)}\,.$$

This relation is very convenient to analyse the structure of the discussed impact factor.

The quantity $A^{(\Lambda)}$ has the same structure as the impact factor for the single bremsstrahlung (1.61) and contains similar vertices, but for photon helicities $\Lambda = 0, \pm1$ and photon virtuality $k^2 \neq 0$. To obtain these vertices, we return to (4). The numerator of the spinor propagator $\hat{p} \pm m$ in (4) consists in two terms. The first term corresponds to the simple replacements

$$\hat{p} + m \to u_{\mathbf{p}}^{(\lambda)}\,\bar{u}_{\mathbf{p}}^{(\lambda)}\,,\;\; \hat{p} - m \to v_{\mathbf{p}}^{(\lambda)}\,\bar{v}_{\mathbf{p}}^{(\lambda)} \tag{14}$$

and leads to the vertex (1.43)

$$V(p) \equiv V_{\lambda\lambda'}(p) = \bar{u}_{\mathbf{p}'}^{(\lambda')}\,\hat{e}_q\,u_{\mathbf{p}}^{(\lambda)} = \bar{v}_{\mathbf{p}}^{(\lambda)}\,\hat{e}_q\,v_{\mathbf{p}'}^{(\lambda')}$$

$$= \sqrt{2}\,\frac{E'}{E_1}\,\delta_{\lambda\lambda'}\,\Phi \tag{15}$$

(with $E' = E$) and to the vertex

$$V(p,\,k) \equiv V_{\lambda\lambda'}^{\Lambda}(p,\,k)$$

$$= \bar{u}_{\mathbf{p}'}^{(\lambda')}\;\hat{e}^{(\Lambda)\,*}(k)\;u_{\mathbf{p}}^{(\lambda)} = \bar{v}_{\mathbf{p}}^{(\lambda)}\;\hat{e}^{(\Lambda)\,*}(k)\;v_{\mathbf{p}'}^{(\lambda')}$$

$$= \left\{\left[\delta_{\lambda\lambda'}\,2\,\left(e^{(\Lambda)\,*}p\right)\,(1 - x\,\delta_{\Lambda,-2\lambda})\right.\right.$$

$$\left.+\,\delta_{\lambda,-\lambda'}\,\delta_{\Lambda,2\lambda}\,\sqrt{2}\,mx\right]\,(1 - \delta_{\Lambda,0})$$

$$\left.+\,2\sqrt{k^2}\,\frac{1-x}{x}\,\delta_{\lambda\lambda'}\,\delta_{\Lambda,0}\right\}\Phi\,. \tag{16}$$

Here $x = \omega/E$ and the function Φ is the same as in (1.41):

$$\Phi = \sqrt{\frac{E}{E'}}\mathrm{e}^{\mathrm{i}(\lambda'\varphi' - \lambda\varphi)}\,. \tag{17}$$

For helicity states $\Lambda = \pm1$ the vertex (16) coincides with that given in (1.39)[2]. It is convenient to present the vertices (15)—(16) by diagrams of Figs. 3 and 4, respectively.

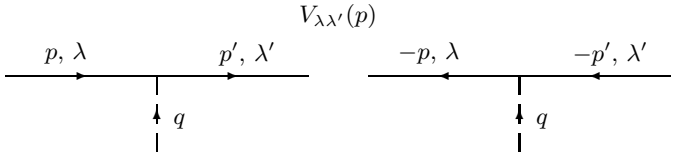

Fig. 3. Vertex $V(p)$ for initial electron (positron) with momentum p and helicity λ, final electron (positron) with p' and λ' and t-channel virtual photon with momentum q and "effective polarization vector" $e_q = \sqrt{2}P_2/s$

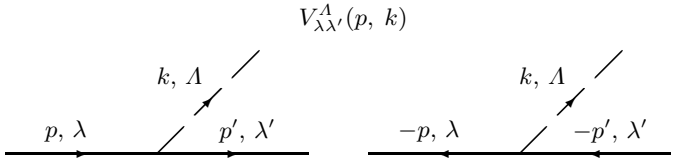

Fig. 4. Vertex $V(p,\,k)$ for initial electron (positron) with p and λ, final electron (positron) with p' and λ' and final photon with k and $\Lambda = 0, \pm1$

The second term in $\hat{p} \pm m$ of (4) corresponds to the more complicated replacements [cf. (1.32)]

$$\hat{p} + m \to \frac{p^2 - m^2}{4E^2}\,v_{-\mathbf{p}}^{(\lambda)}\bar{v}_{-\mathbf{p}}^{(\lambda)} \approx \frac{p^2 - m^2}{4EE_2}\,\hat{P}_2\,,$$

$$\hat{p} - m \to \frac{p^2 - m^2}{4E^2}\,u_{-\mathbf{p}}^{(\lambda)}\bar{u}_{-\mathbf{p}}^{(\lambda)} \approx \frac{p^2 - m^2}{4EE_2}\,\hat{P}_2\,. \tag{18}$$

Since these expressions contain a factor proportional to the denominator of the spinor propagator, that denominator is cancelled and a new vertex with four external lines can be introduced (similar to a vertex with four external particles in scalar QED). Graphically we denote this vertex by the diagrams of Fig. 5 in which the crossed lepton line represents the contracted line corresponding to replacement (18). Using this newly defined vertex, we can avoid from now on vertices $\widetilde{V}$ used in [1].

[2] In the corresponding formulae of [1] there are misprints: in (1.38) and in the equation after (1.36) an additional "minus" sign has to be inserted before the last equality; in (1.40) the factor $-\Lambda$ has to be eliminated; both signs "minus" have to be removed in (1.54); in (1.85), (1.87), (1.104), (1.105) each product of two vertices $\widetilde{V}(p,\,k)$ should be taken with opposite sign.

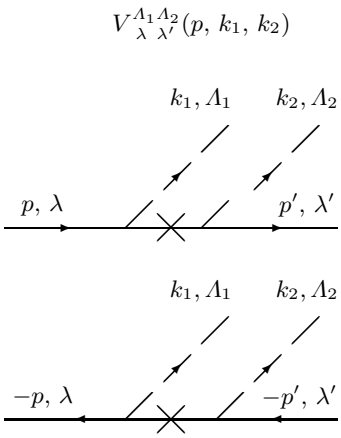

Fig. 5. Vertex $V(p,k_1,k_2)$ for initial and final electrons (positrons) with p, λ and p', λ' and emission of two photons with k_1, Λ_1 and k_2, Λ_2 connected by an crossed intermediate lepton line

The vertex of Fig. 5 is given by

$$\begin{aligned} & V(p,k_1,k_2) \equiv V^{\Lambda_1\Lambda_2}_{\lambda\ \lambda'}(p,k_1,k_2) \\ &= \frac{1}{4(E-\omega_1)E_2}\,\bar{u}^{(\lambda')}_{\mathbf{p}'}\;\hat{e}^{(\Lambda_2)*}(k_2)\;\hat{P}_2\;\hat{e}^{(\Lambda_1)*}(k_1)\;u^{(\lambda)}_{\mathbf{p}} \\ &= \frac{1}{4(E-\omega_1)E_2}\,\bar{v}^{(\lambda)}_{\mathbf{p}}\;\hat{e}^{(\Lambda_1)*}(k_1)\;\hat{P}_2\;\hat{e}^{(\Lambda_2)*}(k_2)\;v^{(\lambda')}_{\mathbf{p}'} \\ &= -2\frac{E'}{E-\omega_1}\,\delta_{\lambda\lambda'}\delta_{\Lambda_1,2\lambda}\,\delta_{\Lambda_1,-\Lambda_2}\Phi. \end{aligned} \tag{19}$$

This equation can be easily proved if we notice that for the used polarization vectors (9) and (12) we have

$$\begin{aligned} & \hat{e}^{(\Lambda_2)*}(k_2)\;\hat{P}_2\;\hat{e}^{(\Lambda_1)*}(k_1) \\ &\qquad = \hat{e}^{(\Lambda_2)*}_{\perp}\;\hat{P}_2\;\hat{e}^{(\Lambda_1)*}_{\perp}\;(1-\delta_{\Lambda_1,0})\;\delta_{\Lambda_1,-\Lambda_2} \\ &\qquad = -\hat{P}_2\;(1+\Lambda_1\,\Sigma_z)\;\delta_{\Lambda_1,\pm1}\,\delta_{\Lambda_2,\mp1}\,, \end{aligned} \tag{20}$$

where the matrix Σ_z is diagonal in the standard as well as in the spinor representation

$$\Sigma_z = \begin{pmatrix} \sigma_z & 0 \\ 0 & \sigma_z \end{pmatrix},$$

σ_z is the Pauli matrix.

In the spirit of paper[1], we can introduce the following additional diagrammatic rules:

1. A crossed lepton line cannot start or end at a vertex with the t-channel virtual photon of momentum q or a virtual photon in the considered jet with helicity state $\Lambda = 0$ (other helicity states for virtual photons of the jet are allowed).
2. Two crossed lines should be separated at least by one uncrossed line. In other words, vertices with more than four external lines are forbidden.

Those rules are due to the fact that a crossed line corresponds to replacements (18). Therefore, rule (1) is due to the equations $\hat{e}_q\,\hat{P}_2 = \hat{P}_2\,\hat{e}_q = 0$ with $e_q = \sqrt{2}P_2/s$ and $\hat{e}^{(0)}\,\hat{P}_2 = \hat{P}_2\,\hat{e}^{(0)} = 0$. Rule (2) is a consequence of the equation $\hat{P}_2\,\hat{e}^{(\Lambda)}(k)\,\hat{P}_2 = 0$.

Now we consider the current $I^{(\Lambda)}$ (6) which is a new vertex corresponding to the transitions $\gamma(k) \to \mu^+(p_+)+\mu^-(p_-)$ or $\gamma(k) \to e^+(p_+)+e^-(p_-)$ with $k = p_+ + p_-$ (Fig. 6):

$$\overline{V}(k,\,p_+) \equiv I^{(\Lambda)} = \overline{V}^{\Lambda}_{\lambda_+\lambda_-}(k,\,p_+) = \bar{u}^{(\lambda_-)}_{\mathbf{p}_-}\;\hat{e}^{(\Lambda)}(k)\;v^{(\lambda_+)}_{\mathbf{p}_+}\,. \tag{21}$$

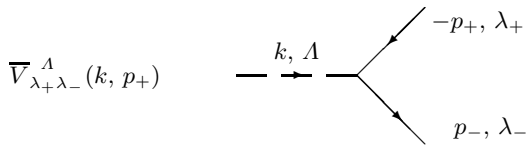

Fig. 6. Vertex $\overline{V}(k,\,p_+)$ for initial photon $(k,\,\Lambda)$ and final lepton $(p_-,\,\lambda_-)$ and antilepton $(p_+,\,\lambda_+)$

Let us compare this vertex with $V(p,\,k)$ from (16). Taking into account that

$$e^{(\Lambda)}_{\perp} = -e^{(-\Lambda)\,*}_{\perp},\;\; e^{(0)}(k) = -e^{(0)}(-k)\,,$$

we find

$$e^{(\Lambda)}(k) = -e^{(-\Lambda)\,*}(-k)\,. \tag{22}$$

In addition, it is known (see Appendix in [1]) that the bispinor $v^{(\lambda_+)}_{\mathbf{p}_+}$ can be obtained from the bispinor $u^{(\lambda)}_{\mathbf{p}}$:

$$v^{(\lambda_+)}_{\mathbf{p}_+} = u^{(\lambda)}_{\mathbf{p}}(E \to -E_+,\,\lambda \to -\lambda_+,\,\theta \to \theta_+,\,\varphi \to \varphi_+) \tag{23}$$

with the convention $\sqrt{-E_+} = +\mathrm{i}\sqrt{E_+}$. Due to these connections between spinors and polarization vectors, we find the useful relation

$$\overline{V}^{\Lambda}_{\lambda_+\lambda_-}(k,\,p_+) = -V^{-\Lambda}_{-\lambda_+\lambda_-}(-p_+,\,-k) \tag{24}$$

from which it immediately follows that

$$\begin{aligned} & \overline{V}^{\ \Lambda}_{\lambda_+\lambda_-}(k,\,p_+) \\ &= \mathrm{i}\left\{\frac{1}{x_+}\left[\delta_{\lambda_+,-\lambda_-}\;2\;\left(e^{(\Lambda)}p_+\right)\;\left(\delta_{\Lambda,-2\lambda_+}-x_+\right)\right.\right. \\ &\quad \left.-\delta_{\lambda_+\lambda_-}\;\delta_{\Lambda,2\lambda_+}\;\sqrt{2}\,m\right]\;(1-\delta_{\Lambda,0}) \\ &\quad \left.+2\,\sqrt{k^2}\,x_-\,\delta_{\lambda_+,-\lambda_-}\;\delta_{\Lambda,0}\right\}\overline{\Phi}\,, \end{aligned} \tag{25}$$

where

$$x_\pm = \frac{E_\pm}{\omega}\,,\quad \overline{\Phi} = \sqrt{\frac{E_+}{E_-}}\,\mathrm{e}^{\mathrm{i}(\lambda_+\varphi_+ + \lambda_-\varphi_-)}\,. \tag{26}$$

It is useful to recall that for the polarization vectors we have

$$e^{(\pm)}p_+ = e_\perp^{(\pm)}\,(p_{+\perp} - x_+ k_\perp) = -e^{(\pm)}p_- = -e_\perp^{(\pm)}\,(p_{-\perp} - x_- k_\perp)\,. \quad (27)$$

Using (27) and the equalities $x_+ + x_- = 1$, $k_\perp = p_{+\perp} + p_{-\perp}$, we can rewrite (25) in the form

$$\overline{V}^{\,\Lambda}_{\lambda_+\lambda_-}(k,\,p_+) = \mathrm{i}\,\sqrt{E_+E_-} \times\Bigg\{\Bigg[2\delta_{\lambda_+,-\lambda_-}e_\perp^{(\Lambda)}\left(\frac{p_{+\perp}}{E_+}\delta_{\Lambda,-2\lambda_+} + \frac{p_{-\perp}}{E_-}\delta_{\Lambda,-2\lambda_-} - \frac{k_\perp}{\omega}\right) -\delta_{\lambda_+\lambda_-}\,\delta_{\Lambda,2\lambda_+}\,\sqrt{2}\,\frac{m\omega}{E_+E_-}\Bigg]\,(1-\delta_{\Lambda,0}) +2\frac{\sqrt{k^2}}{\omega}\,\delta_{\lambda_+,-\lambda_-}\,\delta_{\Lambda,0}\Bigg\}\,\mathrm{e}^{\mathrm{i}(\lambda_+\varphi_+ + \lambda_-\varphi_-)}, \quad (28)$$

which clearly exhibits the symmetry under lepton exchange $e^+ \leftrightarrow e^-$:

$$\overline{V}^{\,\Lambda}_{\lambda_+\,\lambda_-}(k,\,p_+) = \overline{V}^{\,\Lambda}_{\lambda_-\,\lambda_+}(k,\,p_-)\,. \quad (29)$$

Analogously to (19), it is convenient to introduce vertices with four external lines obtained from diagrams of Fig. 5 by interchanging one of the outgoing photons with the initial lepton or antilepton. For example, performing the replacements $k_1 \to -k_1$, $\Lambda_1 \to -\Lambda_1$, $p \to -p$, $\lambda \to -\lambda$ we get

$$\begin{aligned}\overline{V}(k_1,\,p,\,k_2) &\equiv \overline{V}^{\,\Lambda_1\Lambda_2}_{\lambda\;\lambda'}(k_1,\,p,\,k_2)\\ &= \frac{1}{4(\omega_1-E)E_2}\,\bar{u}^{(\lambda')}_{\mathbf{p}'}\,\hat{e}^{(\Lambda_2)*}(k_2)\,\hat{P}_2\,\hat{e}^{(\Lambda_1)}(k_1)\,v^{(\lambda)}_{\mathbf{p}}\\ &= \frac{1}{4(\omega_1-E)E_2}\,\bar{u}^{(\lambda)}_{\mathbf{p}}\,\hat{e}^{(\Lambda_1)}(k_1)\,\hat{P}_2\,\hat{e}^{(\Lambda_2)*}(k_2)\,v^{(\lambda')}_{\mathbf{p}'}\\ &= 2\mathrm{i}\frac{E'}{\omega_1-E}\,\delta_{\lambda,-\lambda'}\,\delta_{\Lambda_1,2\lambda}\,\delta_{\Lambda_1,\Lambda_2}\,\sqrt{\frac{E}{E'}}\,\mathrm{e}^{\mathrm{i}(\lambda\varphi+\lambda'\varphi')}\,. \quad (30)\end{aligned}$$

The last identity in this equation can be easily obtained using a relation analogous to (24):

$$\overline{V}^{\,\Lambda_1\Lambda_2}_{\lambda\;\lambda'}(k_1,\,p,\,k_2) = -V^{-\Lambda_1\Lambda_2}_{-\lambda\;\lambda'}(-p,\,-k_1,\,k_2)\,. \quad (31)$$

Furthermore, we can specify equation (30) for the two diagrams of Fig. 7 which represent the two possible crossings of the diagrams of Fig. 5: either

$$\overline{V}^{\,\Lambda\Lambda'}_{\lambda_+\lambda_-}(k,\,p_+,\,k') = 2\mathrm{i}\,\frac{\sqrt{E_+E_-}}{\omega-E_+}\,\delta_{\lambda_+,-\lambda_-}\,\delta_{\Lambda,2\lambda_+}\,\delta_{\Lambda\Lambda'}\,\mathrm{e}^{\mathrm{i}(\lambda_+\varphi_+ + \lambda_-\varphi_-)} \quad (32)$$

or

$$\overline{V}^{\,\Lambda\Lambda'}_{\lambda_-\lambda_+}(k,\,p_-,\,k') = 2\mathrm{i}\,\frac{\sqrt{E_+E_-}}{\omega-E_-}\,\delta_{\lambda_+,-\lambda_-}\,\delta_{\Lambda,2\lambda_-}\,\delta_{\Lambda\Lambda'}\,\mathrm{e}^{\mathrm{i}(\lambda_+\varphi_+ + \lambda_-\varphi_-)}\,. \quad (33)$$

The further calculation of the discussed impact factor (5) will be performed in Sect. 4.

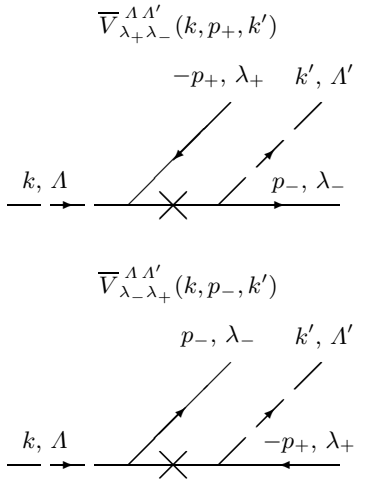

Fig. 7. Vertices $\overline{V}(k,\,p_+,k')$ and $\overline{V}(k,\,p_-,k')$ for the transition of initial photon $(k,\,\Lambda)$ to final electron (or positron) with emission of positron (or electron) and photon $(k',\,\Lambda')$ connected by an crossed intermediate lepton line

2.2 Some properties of the vertex $\overline{V}(k,\,p_+)$

For reference reasons it is useful to present formulae (25) for some particular cases, omitting the factors $\overline{\Phi}$. In the case of the helicity conserved transitions, $\lambda_+ = -\lambda_-$, these vertices are of the form:

$$\begin{aligned}&\overline{V}(k,p_+) = -2\mathrm{i}\,ep_+ && \text{for}\;\; \Lambda = 2\lambda_+ = -2\lambda_-\,,\\ &\overline{V}(k,p_+) = \frac{2\mathrm{i}}{x_+}\,(1-x_+)\,ep_+ && \text{for}\;\; \Lambda = -2\lambda_+ = 2\lambda_-\,,\\ &\overline{V}(k,p_+) = 2\mathrm{i}\sqrt{k^2}\,x_- && \text{for}\;\; \Lambda = 0\,. \end{aligned} \quad (34)$$

In the case of the helicity non-conserved transitions, $\lambda_+ = \lambda_-$, we have:

$$\begin{aligned}&\overline{V}^{\,+}_{++}(k,p_+) = \overline{V}^{\,-}_{--}(k,p_+) = -\frac{\sqrt{2}\,\mathrm{i}}{x_+}\,m\,,\\ &\overline{V}^{\,-}_{++}(k,p_+) = \overline{V}^{\,+}_{--}(k,p_+)\\ &\qquad = \overline{V}^{\,0}_{++}(k,p_+) = \overline{V}^{\,0}_{--}(k,p_+) = 0\,.\end{aligned} \quad (35)$$

The properties of the new vertices are quite similar to those for the previous bremsstrahlung vertices. In particular, vertices with the maximal change of helicity

$$\max|\Delta\lambda| = \max|\Lambda - \lambda_+ - \lambda_-| = 2 \quad (36)$$

are absent. If the final $e^\pm$ becomes very hard ($x_\pm \to 1$, $x_\mp \to 0$) the initial photon "transmits" its helicity to this hard lepton, i.e. the vertex $\overline{V}(k,p_+)$ with $\Lambda = 2\lambda_\pm$ dominates at $x_\pm \to 1$. For helicity non-conserved vertices there is a strong correlation between the helicity of the photon and the positron:

$$\Lambda = 2\lambda_+ \quad \text{if} \quad \lambda_+ = \lambda_-\,. \quad (37)$$

2.3 Substitution rules for the cross-channel

Let us consider the direct process of Fig. 8

$$a(p_1) + b(p_2) \to c(k) + \dots \tag{38}$$

and the so-called conjugated or cross-process of Fig. 9

$$\bar{c}(\bar{p}_1) + b(p_2) \to \bar{a}(\bar{k}) + \dots \tag{39}$$

where $\bar{a}$ and $\bar{c}$ denote the corresponding antiparticles. It is well-known that the amplitude $\overline{M}_{fi}$ of the cross-channel can be obtained from the amplitude M_{fi} of the direct process by replacing:

$$p_1 \to -\bar{k}\,,\ \ k \to -\bar{p}_1\,,\ \ \lambda_a \to -\lambda_{\bar{a}}\,,\ \ \lambda_c \to -\lambda_{\bar{c}} \tag{40}$$

(and, may be, by an additional change of sign, cf. (22) and footnote 1.4). In this section the $\lambda_{a,c}$ generically denote the helicities of both leptons and photons.

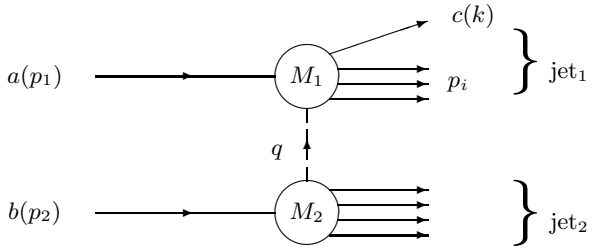

Fig. 8. Generic block diagram of the direct process $a(p_1) + b(p_2) \to c(k) + ... + \text{jet}_2$

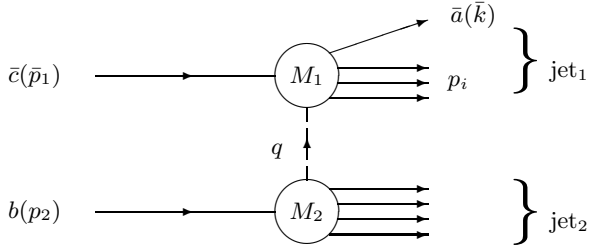

Fig. 9. Generic block diagram of the cross-process $\bar{c}(\bar{p}_1) + b(p_2) \to \bar{a}(\bar{k}) + ... + \text{jet}_2$

If, for example, the considered initial particle is an electron, $a = e^-(p_1)$, and the final particle to be crossed a photon, $c = \gamma(k)$, then $\bar{a} = e^+(\bar{k})$ and $\bar{c} = \gamma(\bar{p}_1)$. The initial electron with 4-momentum p_1 and helicity λ_1 is described by the bispinor $u^{(\lambda_1)}_{\mathbf{p}_1}$ in the amplitude of the direct process. In the conjugated process the particle $\bar{a}$ is the final positron with 4-momentum $\bar{k} \equiv p_+$ and helicity λ_+ described by the bispinor $v^{(\lambda_+)}_{\mathbf{p}_+}$. These bispinors are connected by relation (23). Analogously, the final photon with 4-momentum k and helicity Λ is described by the polarization vector $e^{(\Lambda)*}(k)$ in M_{fi}. For the conjugated process in $\overline{M}_{fi}$ the initial photon with 4-momentum $\bar{p}_1 = -k$ and helicity Λ is described by $e^{(\Lambda)}(-k)$. These polarization vectors are connected by relation (22).

Between the Sudakov variables for the direct and conjugated processes certain relations exist which were obtained in [2]. In the direct process we introduce the Sudakov variables for the initial particle a with 4-momentum p_1, the particle c in the first jet with 4-momentum k and for some other particle in the first jet with p_i, using the definition[3]:

$$k = xP_1 + yP_2 + k_\perp\,,\ \ p_i = x_iP_1 + y_iP_2 + p_{i\perp}\,, \tag{41}$$

$$P_{1,2} = p_{1,2} - \frac{p^2_{1,2}}{s}\,p_{2,1}\,,\ \ P^2_{1,2} = 0\,,\ \ k_\perp p_{1,2} = p_{i\perp}p_{1,2} = 0\,.$$

For the conjugated process we have

$$\bar{k} = \bar{x}\bar{P}_1 + \bar{y}\bar{P}_2 + \bar{k}_\perp\,,\ \ p_i = \bar{x}_i\bar{P}_1 + \bar{y}_i\bar{P}_2 + \bar{p}_{i\perp}\,, \tag{42}$$

$$\bar{P}_{1,2} = \bar{p}_{1,2} - \frac{\bar{p}^2_{1,2}}{\bar{s}}\,\bar{p}_{2,1}\,,\ \ \bar{P}^2_{1,2} = 0\,,\ \ \bar{k}_\perp\bar{p}_{1,2} = \bar{p}_{i\perp}\bar{p}_{1,2} = 0\,.$$

In the jet-like kinematics all particles in the first jet have large components along P_1 in the direct process (or along $\bar{P}_1$ in the conjugated process) and small components along P_2 (or $\bar{P}_2$), therefore, x, x_i, $\bar{x}$, $\bar{x}_i \sim 1$, while $y \sim (k^2 + \mathbf{k}^2_\perp)/s$, $y_i \sim (m_i^2 + \mathbf{p}^2_{i\perp})/s$ and $\bar{y} \sim (k^2 + \bar{\mathbf{k}}^2_\perp)/\bar{s}$, $\bar{y}_i \sim (\bar{m}_i^2 + \bar{\mathbf{p}}^2_{i\perp})/\bar{s}$. Comparing

$$x = \frac{2kP_2}{s} = \frac{kp_2}{p_1p_2}\,,\ \ x_i = \frac{p_ip_2}{p_1p_2}$$

with

$$\bar{x} = \frac{2\bar{k}\bar{P}_2}{\bar{s}} = \frac{p_1p_2}{kp_2}\,,\quad \bar{x}_i = -\frac{p_ip_2}{kp_2}\,,$$

we immediately obtain the relations

$$x = \frac{1}{\bar{x}}\,,\quad x_i = -\frac{\bar{x}_i}{\bar{x}}\,,\quad s = -\bar{s}\bar{x}\,. \tag{43}$$

Presenting the equation $-p_1 = \bar{k} = \bar{x}\bar{P}_1 + \bar{y}\bar{P}_2 + \bar{k}_\perp$ in the form

$$-p_1 = -\bar{x}k + \bar{b}p_2 + \bar{k}_\perp\,,\ \ \bar{b} = \bar{y} - \frac{\bar{x}k^2}{\bar{s}}\,,$$

the 4-vector k from the right-hand-side can be expressed as follows

$$k = \frac{1}{\bar{x}}(p_1 + \bar{b}p_2 + \bar{k}_\perp)\,.$$

Comparing this equation with

$$k = xP_1 + yP_2 + k_\perp = xp_1 + bp_2 + k_\perp\,,\ \ b = y - \frac{xp_1^2}{s}\,,$$

and taking into account (43) and the conditions $k_\perp p_2 = \bar{k}_\perp p_2 = 0$, we obtain

$$k_\perp = \frac{\bar{k}_\perp}{\bar{x}}\,. \tag{44}$$

[3] Formulae given below are valid up to terms of the relative order of $(m_i^2 + \mathbf{p}^2_{i\perp})/s$ or $(\bar{m}_i^2 + \bar{\mathbf{p}}^2_{i\perp})/\bar{s}$ which we systematically omit (here $s = 2p_1p_2\,,\ \ \bar{s} = 2\bar{p}_1\bar{p}_2\,,\ \ \bar{p}_2 = p_2$).

Performing a similar comparison for the 4-momenta of the other particles in the first jet between

$$p_i = \bar{x}_i \bar{P}_1 + \bar{y}_i \bar{P}_2 + \bar{p}_{i\perp} = -\bar{x}_i x p_1 + \bar{b}_i p_2 - \bar{x}_i k_\perp + \bar{p}_{i\perp}$$

and

$$p_i = x_i P_1 + y_i P_2 + p_{i\perp} = x_i p_1 + b_i p_2 + p_{i\perp}\,,$$

we find another useful relation

$$p_{i\perp} = \bar{p}_{i\perp} - \frac{\bar{x}_i}{\bar{x}}\,\bar{k}_\perp\,. \tag{45}$$

As expected, the transformations (43) respect the conservation of energy fraction and (44, 45) the transverse momentum conservation of the direct and conjugated process within the first jet:

$$\begin{aligned} 1 &= x + \sum_i x_i = \bar{x} + \sum_i \bar{x}_i\,,\\ q_\perp &= k_\perp + \sum_i k_{i\perp} = \bar{k}_\perp + \sum_i \bar{k}_{i\perp}\,. \end{aligned}$$

Since the impact factor J_1 of that jet depends only on energy fractions, transverse momenta and helicities of all final particles in the jet and of the incoming particle (energy fraction equal to one, no transverse momentum), the transformations (43-45) together with the helicity changes (40) for the particles to be crossed completely describe the transformation from an impact factor in the direct process to that of the cross-process. Finally, a possible sign change in the impact factor as a result of transformation of the form (22) has to be taken into account.

3 Pair production in γe and $\gamma\gamma$ collisions

The impact factor for the single lepton pair production of Fig. 1.3 can be obtained from (1.61) by the replacements

$$\begin{aligned} &p_1 \to -p_+\,,\ p_3 \to p_-\,,\ k \to -k\,,\\ &e^{(\Lambda)*}(k) \to e^{(\Lambda)}(k)\,,\ \ u_1 \to v_+\,,\ \ u_3 \to u_- \end{aligned} \tag{46}$$

and is of the form

$$J_1(\gamma_\Lambda + \gamma^* \to e^+_{\lambda_+} + e^-_{\lambda_-}) = 4\pi\alpha \left(\frac{N_+}{2kp_+} + \frac{N_-}{2kp_-}\right) \tag{47}$$

$$\begin{aligned} N_+ &= \bar{u}_-\,\hat{e}_q\,(-\hat{p}_+ + \hat{k} + m)\,\hat{e}\,v_+\,,\\ N_- &= \bar{u}_-\,\hat{e}\,(\hat{p}_- - \hat{k} + m)\,\hat{e}_q\,v_+\,, \end{aligned}$$

$e \equiv e^{(\Lambda)}(k)$ is the polarization 4-vector of the initial photon and $e_q = \sqrt{2}P_2/s$. Following along the lepton line and using the rules from Sect. 2.1, the impact factor can be written in the form

$$\begin{aligned} J_1 = 4\pi\alpha\ \Bigg[&\frac{\overline{V}^{\,\Lambda}_{\lambda_+\,\lambda}(k,p_+)V_{\lambda\,\lambda_-}(k-p_+)}{2kp_+}\\ &-\frac{\overline{V}^{\,\Lambda}_{\lambda_-\,\lambda}(k,p_-)V_{\lambda\,\lambda_+}(k-p_-)}{2kp_-}\Bigg], \end{aligned} \tag{48}$$

where the vertices $V(p)$ and $\overline{V}(k,p_\pm)$ are given by (15) and (25), (29), respectively.

In the following we could repeat here all steps of the calculation as described in Sect. 4 of [1]. However, instead of performing the calculations, the final expression can be directly obtained from (1.75), (1.76) using the substitution rules:

$$\begin{aligned} &J_1(e\gamma^* \to e\gamma) \to -\frac{J_1(\gamma\gamma^* \to e^+e^-)}{x_+}\\ &x \to \frac{1}{x_+}\,,\ \frac{k_\perp}{x} \to p_{+\perp}\,,\ \ q_\perp - \frac{k_\perp}{x} \to p_{-\perp}\,,\\ &\lambda_1 \to -\lambda_+\,,\ \lambda_3 \to \lambda_-\,,\ \Lambda \to -\Lambda\,,\ \varphi_1 \to \varphi_+\,,\ \varphi_3 \to \varphi_- \end{aligned} \tag{49}$$

where $x_\pm = E_\pm/\omega$. This gives

$$\begin{aligned} &J_1(\gamma_\Lambda + \gamma^* \to e^+_{\lambda_+} + e^-_{\lambda_-}) =\\ &= 8\pi\alpha\ \mathrm{i}\sqrt{x_+x_-}\,\mathrm{e}^{\mathrm{i}(\lambda_+\varphi_+ + \lambda_-\varphi_-)} \times\\ &\Big[\big(x_+ - \delta_{\Lambda,-2\lambda_+}\big)\,\sqrt{2}\mathbf{T}\mathbf{e}^{(\Lambda)}_\perp \delta_{\lambda_+,-\lambda_-} - mS\delta_{\lambda_+\lambda_-}\delta_{\Lambda,2\lambda_+}\Big]\,. \end{aligned} \tag{50}$$

The transverse 4-vector T (in the used reference frame $T = (0,\mathbf{T},0)$, $T^2 = -\mathbf{T}^2$) and the scalar S are defined as

$$\begin{aligned} &T = \frac{p_{+\perp}}{a} + \frac{p_{-\perp}}{b}\,,\ \ S = \frac{1}{a} - \frac{1}{b}\,,\\ &a = m^2 + \mathbf{p}^2_{+\perp}\,,\ \ b = m^2 + \mathbf{p}^2_{-\perp}\,, \end{aligned} \tag{51}$$

with the useful relation

$$\mathbf{T}^2 + m^2S^2 = \frac{\mathbf{q}^2_\perp}{ab}\,. \tag{52}$$

Since $T \propto q_\perp$ and $S \propto q_\perp$, we conclude that $J_1 \propto q_\perp$. The impact factor (48), (50) changes its sign under the exchange $+ \leftrightarrow -$ which is directly related to the obvious symmetry of diagrams of Fig. 1.3 under lepton exchange $e^+ \leftrightarrow e^-$.

It is interesting to compare the structure of the amplitudes obtained for single bremsstrahlung (Fig. 1.2) and for single pair production (Fig. 1.3). In the former case using (1.63), we can express the amplitude of the inelastic process $ee \to ee\gamma$ via the amplitudes of *one* elastic process $ee \to ee$ but with different momenta for leptons of the upper block:

$$\begin{aligned} &M_{ee\to ee\gamma} = \sqrt{4\pi\alpha}\\ &\Bigg\{\frac{V^{\Lambda}_{\lambda_1\lambda}(p_1,k)}{2kp_1}\,[M_{ee\to ee}(p_1-k,p_3)]_{\lambda\,\lambda_3}\\ &-[M_{ee\to ee}(p_1,p_3+k)]_{\lambda_1\,\lambda}\,\frac{V^{\Lambda}_{\lambda\,\lambda_3}(p_3+k,k)}{2kp_3}\Bigg\}. \end{aligned} \tag{53}$$

This expression can be considered as a generalization of the well-known classical current approximation,

$$M_{ee\to ee\gamma} = \sqrt{4\pi\alpha}\,\left[\frac{p_1e^*}{kp_1} - \frac{p_3e^*}{kp_3}\right] M_{ee\to ee}(p_1,p_3)\,, \tag{54}$$

which is valid for soft photon emission, $\omega \ll E_{1,3}$. On the other hand, Eq. (53) is valid for the emission of a

photon with arbitrary energy but for small angles of the final photon and lepton.

For single pair production an equation analogous to (53) can be directly derived from (48):

$$M_{\gamma e\to l^+l^-e} = \sqrt{4\pi\alpha}$$
$$\left\{ \frac{\overline{V}^{\Lambda}_{\lambda_+\,\lambda}(k,p_+)}{2kp_+}\,[M_{l^-e\to l^-e}(k-p_+,p_-)]_{\lambda\,\lambda_-} \right.$$
$$\left. + \frac{\overline{V}^{\Lambda}_{\lambda_-\,\lambda}(k,p_-)}{2kp_-}\,[M_{l^+e\to l^+e}(k-p_-,p_+)]_{\lambda\,\lambda_+} \right\}. \quad (55)$$

In contrast to the bremsstrahlung case, the amplitude for pair production is expressed via amplitudes for *two different* elastic processes: $l^+e\to l^+e$ and $l^-e\to l^-e$.

Having the impact factors for single bremsstrahlung (1.68) or (1.75) and for single pair production (50), we are able to obtain the amplitudes for the processes of Figs. 1.2–1.6. More details about the double bremsstrahlung in opposite directions of Fig. 1.4 and the double pair production of Fig. 1.5 can be found in Refs. [3] and [4], respectively. In the same manner, using the impact factor for double bremsstrahlung along one direction from Sect. 5 of [1], we get the impact factor for the process of Fig. 1.10, the corresponding calculations can be found in Ref. [5].

4 Pair production in e^+e^- collisions

We start with bremsstrahlung $\mu^+\mu^-$ pair production of Fig. 1.8. The corresponding impact factor is given by the expression (see Sect. 2.1)

$$J_1(e^-_{\lambda_1}+\gamma^*\to e^-_{\lambda_3}+\mu^+_{\lambda_+}+\mu^-_{\lambda_-})$$
$$= -\frac{\sqrt{4\pi\alpha}}{k^2}\sum_{\Lambda=0,\pm1} A^{(\Lambda)}\overline{V}^{\Lambda}(k,p_+)\,. \quad (56)$$

The vertex $\overline{V}(k,p_+)$ has been obtained already in (25) (the mass has to be identified with the muon mass m_μ), the virtuality of the photon $k^2=(p_++p_-)^2$ is given via the energy fractions $x_\pm=E_\pm/E_1$ (with $x_++x_-=x=\omega/E_1$) and transverse momenta $\mathbf{p}_\pm$ (with $\mathbf{p}_{+\perp}+\mathbf{p}_{-\perp}=\mathbf{k}_\perp$) of the muons:

$$k^2=\frac{1}{x_+x_-}\left[x^2m_\mu^2+(x_-\mathbf{p}_{+\perp}-x_+\mathbf{p}_{-\perp})^2\right]. \quad (57)$$

Therefore, it remains to calculate the quantities $A^{(\pm)}$ and $A^{(0)}$ only. Using the rules from Sect. 2.1, we obtain the expression similar to (1.63):

$$A^{(\Lambda)}=4\pi\alpha\left[\frac{V(p_1,k)V(p_1-k)}{2kp_1-k^2}-\frac{V(p_1)V(p_3+k,k)}{2kp_3+k^2}\right],$$

the vertices $V(p)$ and $V(p,k)$ are given by (15) and (16), respectively. Since

$$2kp_1-k^2=xa\,,\quad a=m^2+\frac{\mathbf{k}_\perp^2}{x^2}+\frac{1-x}{x^2}k^2\,,$$

$$2kp_3+k^2=\frac{x}{1-x}\,b\,, \quad (58)$$
$$b=m^2+\left(\mathbf{q}_\perp-\frac{\mathbf{k}_\perp}{x}\right)^2+\frac{1-x}{x^2}k^2\,,$$

where m is the electron mass, we can repeat the derivation of (1.75) with the result

$$A^{(\Lambda)}=8\pi\alpha\frac{\sqrt{1-x}}{x}\,\mathrm{e}^{\mathrm{i}(\lambda_3\varphi_3-\lambda_1\varphi_1)} \quad (59)$$
$$\times\left[(1-x\delta_{\Lambda,-2\lambda_1})\,\sqrt{2}\mathbf{Te}^{(\Lambda)\,*}_{\perp}\,\delta_{\lambda_1\lambda_3}+m\,xS\delta_{\lambda_1,-\lambda_3}\delta_{\Lambda,2\lambda_1}\right]$$

for $\Lambda=\pm1$ and

$$A^{(0)}=8\pi\alpha\frac{\sqrt{1-x}}{x}\,\mathrm{e}^{\mathrm{i}(\lambda_3\varphi_3-\lambda_1\varphi_1)}\,\frac{\sqrt{k^2}}{x}\,S\,\delta_{\lambda_1\lambda_3} \quad (60)$$

for $\Lambda=0$. Here we have used the scalar S and the transverse 4-vector T:

$$S=\frac{1}{a}-\frac{1}{b}\,,\quad T=\frac{(k_\perp/x)}{a}+\frac{q_\perp-(k_\perp/x)}{b}\,. \quad (61)$$

They obey the relation

$$\mathbf{T}^2+\left(m^2+\frac{1-x}{x^2}k^2\right)S^2=\frac{\mathbf{q}_\perp^2}{ab} \quad (62)$$

from which it follows that $J_1\propto q_\perp$.

The final results (56), (59), (60) and (25) coincide with those obtained in [6] by means of considerably more complicated calculations. The impact factor for the cross-channel of Fig. 1.7 can be obtained using the substitution rules, the corresponding expression is given in [6].

5 Bremsstrahlung $\mu^+\mu^-$ pair production with additional photon

In this section we demonstrate how the newly defined rules in the jet-like kinematics can be efficiently applied to the more complicated reaction

$$ee\to ee\mu^+\mu^-\gamma$$

where both the produced muon pair and the photon belong to the first jet. That process (which is shown schematically in Fig. 1) is described by two sets of Feynman diagrams. The first set is the bremsstrahlung $\mu^+\mu^-$ pair production of Fig. 1.8 with an additional photon line attached to the initial electron line and to every muon and electron line in the first jet. The second set is the two-photon $\mu^+\mu^-$ pair production of Fig. 1.7 adding again a photon line to both the initial electron and all final leptons line in the first jet. In this section we consider the first set of diagrams having in mind that the amplitudes for the second set can be obtained by a simple transition to the cross-channel. The impact factor J_1 for the set under discussion is described by the diagrams of Figs. 10 and 11.

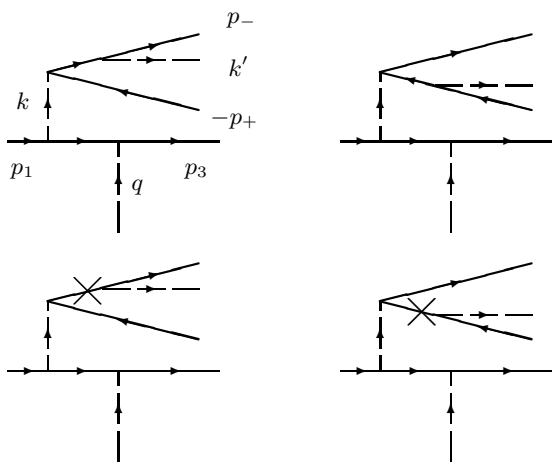

Fig. 10. Diagrams (including crossed intermediate muon lines) for the impact factor related to bremsstrahlung $\mu^+\mu^-$ pair production with an additional photon emitted by muons

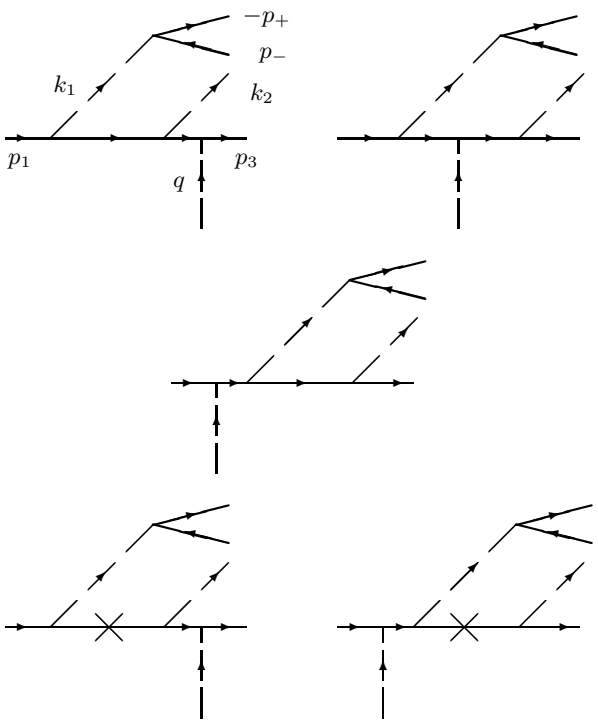

Fig. 11. Diagrams for the impact factor related to bremsstrahlung $\mu^+\mu^-$ pair production with an additional photon emitted by the electron

5.1 Photon emission by muons (Fig. 10)

The contribution of Fig. 10 can be written in the form

$$J_1^{(10)}(e^-_{\lambda_1}+\gamma^*\to e^-_{\lambda_3}+\mu^+_{\lambda_+}+\mu^-_{\lambda_-}+\gamma_{\Lambda'}) = -\frac{1}{k^2}\,A_\mu B^\mu = \frac{1}{k^2}\sum_{\Lambda=0,\pm1} A^{(\Lambda)}B^{(\Lambda)}\,, \tag{63}$$

where $A^{(\Lambda)}$ is given by (59), (60) and $B^{(\Lambda)}$ corresponds to the process $\gamma(k)\to\mu^+(p_+)+\mu^-(p_-)+\gamma(k')$:

$$B^{(\Lambda)} = 4\pi\alpha\left(\frac{N_-}{2p_-k'}-\frac{N_+}{2p_+k'}\right) \tag{64}$$

with

$$N_- = \bar u_-\hat e^{(\Lambda')*}(k')\,(\hat p_- + \hat k' + m_\mu)\,\hat e^{(\Lambda)}(k)\,v_+\,,$$
$$N_+ = \bar u_-\hat e^{(\Lambda)}(k)\,(\hat p_+ + \hat k' - m_\mu)\,\hat e^{(\Lambda')*}(k')\,v_+\,.$$

Here m_μ is the muon mass and

$$2p_\pm k' = \frac{x'}{x_\pm}\left(m_\mu^2+\mathbf{r}_\pm^2\right)\,,\quad \mathbf{r}_\pm = \mathbf{p}_{\pm\perp}-\frac{x_\pm}{x'}\mathbf{k}'_\perp\,,$$
$$x_\pm = \frac{E_\pm}{E_1}\,,\quad x' = \frac{\omega'}{E_1}\,, \tag{65}$$
$$k^2 = \frac{1}{x_+x_-}\left[(x_++x_-)^2\,m_\mu^2+(x_-\mathbf{p}_{+\perp}-x_+\mathbf{p}_{-\perp})^2\right] + \frac{x'}{x_+}\left(m_\mu^2+\mathbf{r}_+^2\right)+\frac{x'}{x_-}\left(m_\mu^2+\mathbf{r}_-^2\right)\,. \tag{66}$$

Using the vertices from Sect. 2.1, we immediately obtain

$$\frac{B^{(\Lambda)}}{4\pi\alpha} = \frac{1}{2p_-k'}\overline{V}^{\,\Lambda}_{\lambda_+\,\lambda}(k,p_+)\,V^{\Lambda'}_{\lambda\lambda_-}(k-p_+,k') - \frac{1}{2p_+k'}\overline{V}^{\,\Lambda}_{\lambda_-\,\lambda}(k,p_-)\,V^{\Lambda'}_{\lambda\lambda_+}(k-p_-,k') + \overline{V}^{\,\Lambda\,\Lambda'}_{\lambda_+\,\lambda_-}(k,p_+,k')-\overline{V}^{\,\Lambda\,\Lambda'}_{\lambda_-\,\lambda_+}(k,p_-,k')\,. \tag{67}$$

The last two items are due to diagrams of Fig. 10 with the crossed intermediate muon line.

For a soft final photon ($x'\ll 1$, $\mathbf{k}'_\perp\to 0$ and $\mathbf{k}'_\perp/x'$ remains finite) we have

$$B^{(\Lambda)} = 4\pi\alpha\,\overline{V}^{\,\Lambda}_{\lambda_+\,\lambda_-}(k,p_+)\left(\frac{e'^{*}p_-}{p_-k'}-\frac{e'^{*}p_+}{p_+k'}\right)\,. \tag{68}$$

This expression corresponds to the approximation of classical currents. In that limit the virtuality k^2 of (66) simplifies to (57).

5.2 Photon emission by electrons (Fig. 11)

It is convenient to use the same notation as for the process of double bremsstrahlung (see Fig. 1.13), but to take into account that the photon k_1 is now virtual with $k_1^2>0$ and its helicity is $\Lambda_1=0,\pm1$. In particular, we introduce the energy fractions

$$x_1=\frac{\omega_1}{E_1}=\frac{E_++E_-}{E_1},\quad x_2=\frac{\omega_2}{E_1}\,,\quad X_3=\frac{E_3}{E_1}\,,$$
$$x_1+x_2+X_3=1\,.$$

The denominators of the propagators in Fig. 11 are expressed via the energy fractions, transverse momenta and

virtuality of the first photon k_1^2 as follows:

$$
\begin{aligned}
&a_j \equiv -(p_1-k_j)^2+m^2\,,\;\; b_j \equiv (p_3+k_j)^2-m^2\,,\\
&a_1 = a_1^0 + \frac{1-x_1}{x_1}\,k_1^2\,,\quad a_2 = a_2^0\,,\\
&b_1 = b_1^0 + \frac{x_1+X_3}{x_1}\,k_1^2\,,\quad b_2 = b_2^0\,,\\
&a_{12}=a_{21}\equiv -(p_1-k_1-k_2)^2+m^2 = a_{12}^0+\frac{X_3}{x_1}\,k_1^2\,,\\
&b_{12}=b_{21}\equiv (p_3+k_1+k_2)^2-m^2 = b_{12}^0+\frac{1}{x_1}\,k_1^2\,,
\end{aligned}
\tag{69}
$$

where we denote by the upper index 0 the quantities in the limit $k_1^2=0$ [given in (1.83)]. The virtuality k_1^2 depends on the energy fractions $x_\pm$ with $x_+ + x_- = x_1$ and the transverse momenta of the muons [see (57)]

$$
k_1^2 = \frac{1}{x_+x_-}\left[x_1^2m_\mu^2 + (x_-\mathbf{p}_{+\perp}-x_+\mathbf{p}_{-\perp})^2\right]. \tag{70}
$$

The contribution, corresponding to Fig. 11, can be written in the form (we indicate explicitly the helicity states Λ_1 (Λ_2) of the virtual (real) photon and the initial and final electrons $\lambda_{1,3}$):

$$
\begin{aligned}
J_1^{(11)} &= -\frac{(4\pi\alpha)^2}{k_1^2} \\
&\times \sum_{\Lambda_1=0,\pm1} \overline{V}^{\Lambda_1}_{\lambda_+\lambda_-}(k_1,p_+)\, C^{\Lambda_1\,\Lambda_2}_{\lambda_1\,\lambda_3}(x_1,x_2,k_{1\perp},k_{2\perp},p_{3\perp})\,,
\end{aligned}
\tag{71}
$$

where $\overline{V}(k_1,p_+)$ is given by (25) identifying $k=k_1$ and $m=m_\mu$. To calculate C, we follow the electron line from left to right in the diagrams of Fig. 11 and write down the corresponding vertices:

$$
\begin{aligned}
C = &\frac{1}{a_1a_{12}}\,V(p_1,k_1)\,V(p_1-k_1,k_2)\,V(p_3-q)\\
&-\frac{1}{a_1b_2}\,V(p_1,k_1)\,V(p_1-k_1)\,V(p_1-k_1+q,k_2)\\
&+\frac{1}{b_{12}b_2}\,V(p_1)\,V(p_1+q,k_1)\,V(p_1-k_1+q,k_2)\\
&-\frac{1}{a_{12}}\,V(p_1,k_1,k_2)\,V(p_3-q)\\
&+\frac{1}{b_{12}}\,V(p_1)\,V(p_1+q,k_1,k_2)\\
&+(k_1\leftrightarrow k_2)\,.
\end{aligned}
\tag{72}
$$

The last two contributions contain the four particle vertices corresponding to two last diagrams of Fig. 11 with the crossed lines. Next we take into account the explicit expression (15) for the vertices $V(p)$, the relations for $V(p,k)$ similar to (1.86), the relation

$$
V(p_1,k_1,k_2) = V(p_1+q,k_1,k_2)
$$

and present C in the form

$$
C = \sqrt{2}\,X_3\,(1+\mathcal{P}_{12})\;M^{\Lambda_1\,\Lambda_2}_{\lambda_1\,\lambda_3}(x_1,x_2,k_{1\perp},k_{2\perp},p_{3\perp})\,\Phi_{13}\,. \tag{73}
$$

Here we have introduced the permutation operator $\mathcal{P}_{12}$ and the factor

$$
\Phi_{13} = \frac{1}{\sqrt{X_3}}\,\mathrm{e}^{\mathrm{i}(\lambda_3\varphi_3-\lambda_1\varphi_1)} \tag{74}
$$

including the common phase. This allows us to omit below all factors Φ from vertices $V(p,k)$ and $V(p,k_1,k_2)$. As a result, we obtain the expression similar to (1.87), but with $\Lambda_1=0,\pm1$:

$$
\begin{aligned}
X_3M^{\Lambda_1\Lambda_2}_{\lambda_1\,\lambda_3} &= A_2\,V^{\Lambda_1}_{\lambda_1\lambda}(p_1,k_1)\,V^{\Lambda_2}_{\lambda\lambda_3}(p_1-k_1+q,k_2)\\
&+q_\perp B_2{}^{\Lambda_1\Lambda_2}_{\lambda_1\,\lambda_3}+\widetilde{A}_2V^{\Lambda_1\Lambda_2}_{\lambda_1\lambda_3}(p_1,\,k_1,\,k_2)\,,
\end{aligned}
\tag{75}
$$

where the quantities A_2 and $\widetilde{A}_2$ are of the same form as in (1.88), however with denominators a_1, b_1, a_{12} and b_{12} of the propagators depending on the virtuality k_1^2:

$$
A_2 = \frac{X_3}{a_1a_{12}}-\frac{1-x_1}{a_1b_2}+\frac{1}{b_{12}b_2}\,,\quad \widetilde{A}_2 = -\frac{X_3}{a_{12}}+\frac{1}{b_{12}}\,. \tag{76}
$$

The transverse 4-vector B_2 is similar to that in (1.89):

$$
\begin{aligned}
B_2{}^{\Lambda_1\Lambda_2}_{\lambda_1\,\lambda_3} = &-X_3\,\frac{2e_\perp^{(\Lambda_2)\,*}}{a_1a_{12}}\,V^{\Lambda_1}_{\lambda_1\lambda_3}(p_1,k_1)\\
&\times\left(1-\frac{x_2}{1-x_1}\,\delta_{\Lambda_2,-2\lambda_3}\right)\\
&+\frac{2e_\perp^{(\Lambda_1)\,*}}{b_{12}b_2}\,V^{\Lambda_2}_{\lambda_1\lambda_3}(p_1-k_1+q,k_2)\\
&\times(1-x_1\,\delta_{\Lambda_1,-2\lambda_1})\;(1-\delta_{\Lambda_1,0})\,.
\end{aligned}
\tag{77}
$$

For the case $\Lambda_1=\pm1$ all independent helicity states of amplitude $M^{\Lambda_1\Lambda_2}_{\lambda_1\,\lambda_3}$ from (75) coincide with those in (1.92)–(1.96). For the case $\Lambda_1=0$ we obtain

$$
\begin{aligned}
X_3M^{0\Lambda_2}_{\lambda_1\,\lambda_3} = 2\sqrt{2k_1^2}\,\frac{1-x_1}{x_1}\Bigg[&A_2\,V^{\Lambda_2}_{\lambda_1\lambda_3}(p_1-k_1,k_2)\\
&-\frac{X_3}{a_1a_{12}}\left(q_\perp e_\perp^{(\Lambda_2)\,*}\right)\left(1-\frac{x_2}{1-x_1}\,\delta_{\Lambda_2,-2\lambda_3}\right)\delta_{\lambda_1,\lambda_3}\Bigg]\,.
\end{aligned}
\tag{78}
$$

The amplitudes (75), (78) are given in such a form that all individual large (compared to $q_\perp$) contributions have been rearranged into finite expressions. To show that the impact factor $J_1^{(11)}\propto q_\perp$, it is sufficient to check that the quantities A_2 and $\widetilde{A}_2$ vanish in the limit of small $q_\perp$:

$$
A_2\propto q_\perp\,,\;\; \widetilde{A}_2\propto q_\perp\,. \tag{79}
$$

This could be done by a direct substitution of the expressions for the denominators (69) into (76).

However, it is much easier to be proved using the following simple consideration. Since $x_q = 2qP_2/s \sim m^2/s$ and $y_q = 2qP_1/s\sim m^2/s$, the quantity $q^2 = sx_qy_q+q_\perp^2\approx q_\perp^2$ tends to zero in the limit $q_\perp\to0$. Therefore, in this limit we have

$$
\begin{aligned}
a_{12} = 2p_3q-q^2\to X_3sy_q,\qquad b_{12} = 2p_1q+q^2\to sy_q,\\
a_{12}\to X_3b_{12}\,.
\end{aligned}
\tag{80}
$$

Taking into account

$$a_1 = -(p_3 + k_2 - q)^2 + m^2 \to -b_2 + (1 - x_1) s y_q \quad (81)$$

this leads to

$$\begin{aligned} \widetilde{A}_2 &\to 0\,, \\ A_2 &\to \frac{1}{a_1 s y_q} - \frac{1 - x_1}{a_1 b_2} + \frac{1}{s y_q b_2} \\ &\propto b_2 - (1 - x_1) s y_q + a_1 \to 0\,. \end{aligned} \quad (82)$$

6 Summary

In the present paper we continued to develop a new effective method for calculating all helicity amplitudes of jet-like QED processes at tree level.

Using the jet-like kinematics, the scattering amplitudes are represented in the simple factorized form (2), where the impact factors J_1 or J_2 are proportional to the scattering amplitudes of the first or second initial particle (lepton, antilepton, photon) with the virtual t-channel photon connecting the two impact factors. The final particles in those two produced "jets" have emission and scattering angles much less than unity, though they are allowed to be of the order of typical emission angles m_i/E_i or larger.

In calculating the impact factors in our kinematics we have replaced the spinor structure involving leptons or antileptons of small virtuality by transition vertices which are matrices with respect to incoming and outgoing lepton helicities. These vertices are finite in the limit $s \to \infty$.

In our previous paper we have considered multiple photon bremsstrahlung. In that case the impact factors are given as simple matrix products of vertices going along the lepton line. One generic vertex describes the coupling of the leptons to the t-channel virtual photon. At most two other nonzero such vertices were needed to describe all processes with only real bremsstrahlung photons. At this stage the diagrams of Figs. 1.2, 1.4, 1.9 and 1.11 could be easily calculated including all helicity states.

In the present paper we extended our method to consider also processes with lepton pair production. In other words, we now allow that more than one lepton line connected by virtual photons (with finite energy fraction and small virtuality) are present in the considered impact factor.

The idea based on gauge invariance consists in decomposing the impact factor with such a virtual photon k with helicity Λ into a product of two building blocks $A^{(\Lambda)}$ and $B^{(\Lambda)}$ (which contain their own lepton lines) and sum over the helicities of the virtual photon:

$$J_1 = \frac{1}{k^2} A_\mu B^\mu = -\frac{1}{k^2} \sum_{\Lambda = 0, \pm 1} A^{(\Lambda)} B^{(\Lambda)}. \quad (83)$$

The block $A^{(\Lambda)} = A e^{(\Lambda)*}$ contains the "outgoing", $B^{(\Lambda)} = B e^{(\Lambda)}$ — the "incoming" virtual photon.

For that purpose we have generalized our previous bremsstrahlung vertices to include the case of virtual photons, the corresponding expressions are given in (16). Using simple crossing relations we found the vertices for the $\gamma(k) \to e^+(p_+) + e^-(p_-)$ transition where the initial photon is either real or virtual, the results are collected in (25) and (28). We have also introduced vertices with four external lines (19), (30)—(33) (analogous to the case of scalar QED) for the $e(p) \to [\gamma(k_1)\gamma(k_2)] + e(p')$ as well as the $\gamma(k) \to [e^+(p_+)\gamma(k')] + e^-(p_-)$ and $\gamma(k) \to [e^-(p_-)\gamma(k')] + e^+(p_+)$ transitions. Using these vertices we develop the convenient diagrammatic rules presented in Figs. 3—7.

To discuss the impact factor for the case where initial photons and final leptons or initial leptons and final photons are interchanged we have presented the corresponding crossing rules in (43)–(45). So, e.g., the impact factor of diagram of Fig. 1.10 is the cross channel of the double bremsstrahlung impact factor of Fig. 1.9.

Let us recall again, that the impact factors are finite in the high-energy limit: they depend on the energy fractions and the transverse momenta of the jet particles, and on the helicities of all initial and final particles. By construction all individual large contributions (compared to $q_\perp$) are arranged into finite expressions. Therefore, these helicity amplitudes are very convenient for numerical calculations in the jet-like kinematics.

We have applied our technique to calculate the impact factor for the single lepton pair production of Fig. 1.3, see (50). This allows to obtain the pair production processes shown in Figs. 1.3 and 1.5. Taking into account also the impact factors for single bremsstrahlung, the diagram of Fig. 1.6 is captured too.

The impact factor for the pair production of Fig. 1.8 has been studied in Sect. 4, see (56), (59), (60). Using the crossing relations, also the reaction of Fig. 1.7 is described.

Finally we demonstrated in Sect. 5 how our new method can be used to calculate the leading contribution to higher order impact factors taking as an example a jet from an electron containing in addition a muon pair and a photon. This impact factor can be used to describe the process of Fig. 1.

Acknowledgements

We are grateful to S. Brodsky and A. Vainshtein for useful discussions. This work is supported in part by INTAS (code 00-00679) and by RFBR (code 03-02-17734).

References

1. C. Carimalo, A. Schiller, V.G. Serbo, Eur. Phys. J. C **2**3, 633 (2002)
2. E.A. Kuraev, L.N. Lipatov, M.I. Strikman, Zh. Eksp. Teor. Fiz. **6**6, 838 (1974)
3. E.A. Kuraev, A. Schiller, V.G. Serbo, Z. Phys. C **3**0, 237 (1986)
4. E.A. Kuraev, A. Schiller, V.G. Serbo, Nucl. Phys. B **2**56, 189 (1985)
5. E.A. Kuraev, A. Schiller, V.G. Serbo, B.G. Shaikhatdenov, Nucl. Phys. B **5**70, 359 (2000)
6. E.A. Kuraev, A. Schiller, V.G. Serbo, D.V. Serebryakova, Eur. Phys. J. C **4**, 631 (1998)